BULLETIN OF THE EARTHQUAKE
RESEARCH INSTITUTE
Vol. 57 (1982), pp. 653-686

30. *Mapping of an Unusual Crustal Discontinuity by Microearthquake Reflections in the Earthquake Swarm Area near Ashio, Northwestern Part of Tochigi Prefecture, Central Japan.*

By Megumi MIZOUE, Isao NAKAMURA,

Earthquake Research Institute,

and

Takashi YOKOTA,

Meteorological Research Institute,
Japan Meteorological Agency.

(Received October 30, 1982)

Abstract

Microearthquake seismograms recorded by the stations in the earthquake swarm area near Ashio on the westren border of Tochigi Prefecture, Central Japan, frequently have two sharp phases following the direct S-wave. They were identified as near vertical S to P-wave (S_xP) and S to S-wave (S_xS) reflections from an unusual deep crustal discontinuity. Reflection points calculated on the basis of hypocentral coordinates in combination with the traval time data of the reflections were mapped with contour lines of a 1 km interval. The discontinuity was estimated to have a depth of about 14 km beneath Ashio dipping southeastward with considerable local irregularities. The ratio of observed amplitudes of S_xP to S_xS varies from 0.045 to 0.34 for the incident angle of less than 23°. The theoretical amplitude ratio of the reflections agrees well with the observational results when the S-wave velocity decreases from 3.35 km/sec to 0.00 km/sec across the discontinuity. A horizontal extension of the unusual discontinuity strikes in a NE-SW direction along the general trend of the volcanic front in the area. It is suggested from the analysis that the discontinuity is underlain by a material of very low rigidity and the existence of an extensive magma body may be a plausible explanation of the reflections.

1. Introduction

Most earthquakes near Ashio, Tochigi Prefecture in the northern Kanto district, have occurred in swarm as found by temporary microearthquake observations (KAMINUMA et al., 1970; SUZUKI and KAMEYAMA, 1972; SUZUKI et al., 1973). The local activity in the area is one of the typical examples of earthquake swarms occurring in and around the geothermal or volcanic zones extending from the northern part of Tochigi Prefecture to Fukushima Prefecture, Northeastern Japan (SEKIYA, 1973). Earthquakes occurring near Ashio mostly have a magnitude M of less than 3.0 and no earthquakes with a M of more than 5.0 have been experienced in the area for decades.

Microearthquake observations with a local tripartite network from August, 1972 to March, 1973 disclosed very shallow microearthquakes distributed with a linear arrangement trending in a NE-SW direction (OGINO, 1974). In addition to the characteristic mode of epicentral distribution, it was noted that the nearby earthquakes of the S minus P time of less than 1.5 sec frequently produced two sharp arrivals following the direct S by about 2.5-3.0 sec and 4.5-5.0 sec, respectively. These phases were identified to be near vertical S to P-wave (S_xP) and S to S-wave (S_xS) reflections from the deep crustal discontinuity at a depth of about 14-17 km. Ratios of S_xP to S_xS amplitudes in conjunction with the plane-wave reflection theory suggested the existence of a zone of very low rigidity beneath the discontinuity (MIZOUE, 1980).

Near vertical crustal reflections registered on microearthquake seismograms in the Rio Grande rift, Socorro, New Mexico, were interpreted as evidence of the unusual discontinuity underlain by magma body at a depth of about 19 km (SANFORD and LONG, 1965; SANFORD et al., 1973, 1977; RINEHART and SANFORD 1981). The first full-scale application of the VIBROSEIS profiling technique to a specific geological problem was initiated in the Rio Grande rift near Socorro in 1975 (OLIVER and KAUFMAN, 1976; SCHILT et al., 1979; BROWN et al., 1980). The result of the surveys corresponds in depth and dip to the unusual discontinuity related to the magma body as inferred from the microearthquake reflections.

An extensive study of the crustal reflections from microearthquakes was made in this paper in comparison with the results obtained in the Rio Grande rift. A temporary telemetering network system with a centralized recording unit was introduced for a precise time markings of seismograms to improve the accuracy of arrival time measurements of

the direct and the reflected waves. A network consisting of four stations was operated for the period from November 1981 to March 1982 and more than 150 microearthquakes were detected in the area near Ashio. The hypocentral determination for the events detected at more than three stations gave a detailed pattern of microearthquake distribution in the area.

The arrival times of high precision for the reflections were analysed in combination with the hypocentral coordinates to determine the depths of the unusual discontinuity related to the reflections. The discontinuity was estimated to have a depth of about 14 km beneath Ashio dipping southeastward with considerable local irregularity. Physical properties of the discontinuity were reexamined on the basis of the newly obtained amplitude data. It was concluded from the study that the reflections observed in the vicinity of Ashio could be attributed to the existence of an unusual discontinuity underlain by a material of very low rigidity. The seismological evidence seems to be coincidental with that obtained in the Rio Grande rift for an extensive sill shaped magma body, though detailed discussions should be reserved for future studies.

2. Network system for microearthquake observation

A temporary microearthquake observation network was set up in the Ashio area in November 1981. The seismograph network covered an area

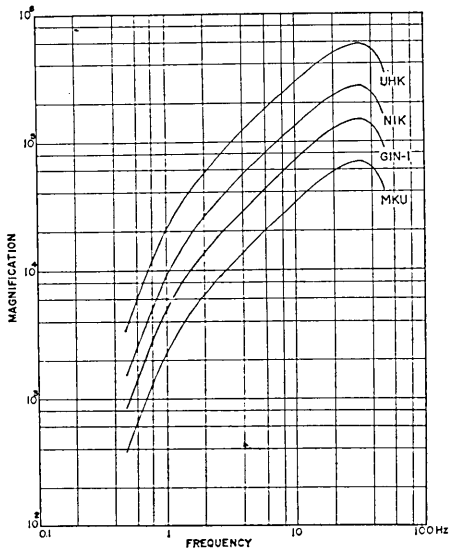

Fig. 1. Overall frequency characteristics of the short period seismographs used.

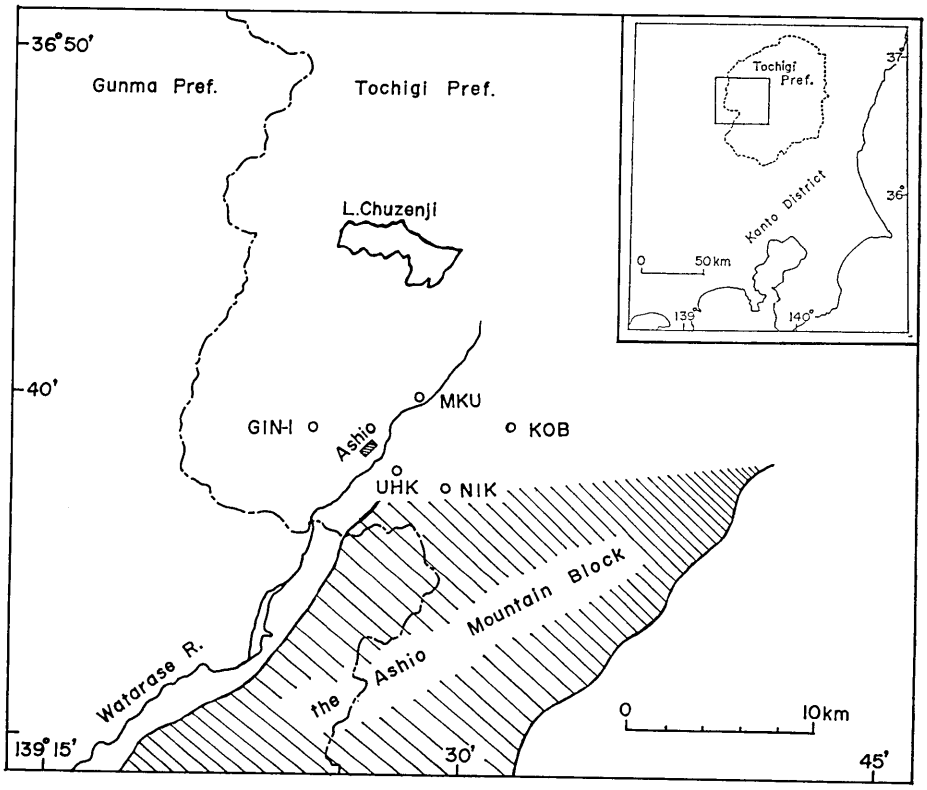

Fig. 2. Location of telemetering seismographic stations for temporary microearthquake observation in the area near Ashio, the northern Kanto district.

of about 5×6 km^2 with four telemetering stations of short period seismographs. The magnification of the seismographs at the stations is given in Fig. 1. The location of the stations is shown in Fig. 2. The Nikko station (NIK) is one of the permanent stations of the regional network covering the Kanto district (Fig. 3) directly linked to the central station of E. R. I. (Earthquake Research Institute, Tokyo University) in Tokyo. Each of the stations has a radio or telephone linked line to transmit seismic waveform data at the rate of 9.6 Kbits/sec. The output of a seismograph is sampled at the rate of 120 samples/sec for 10 bits/sample and transmitted to the central station on real time base with a PCM code. A signal of a 10 bits/sample is converted to a compressed form of 8 bits/sample to increase the number of channels to be transmitted by a line. The compressed form of data is converted to the original form of a 10 bits/sample when recieved at the central station. The radio linked line used for the NIK station has a transmitting capacity of 9.6 Kbits/sec,

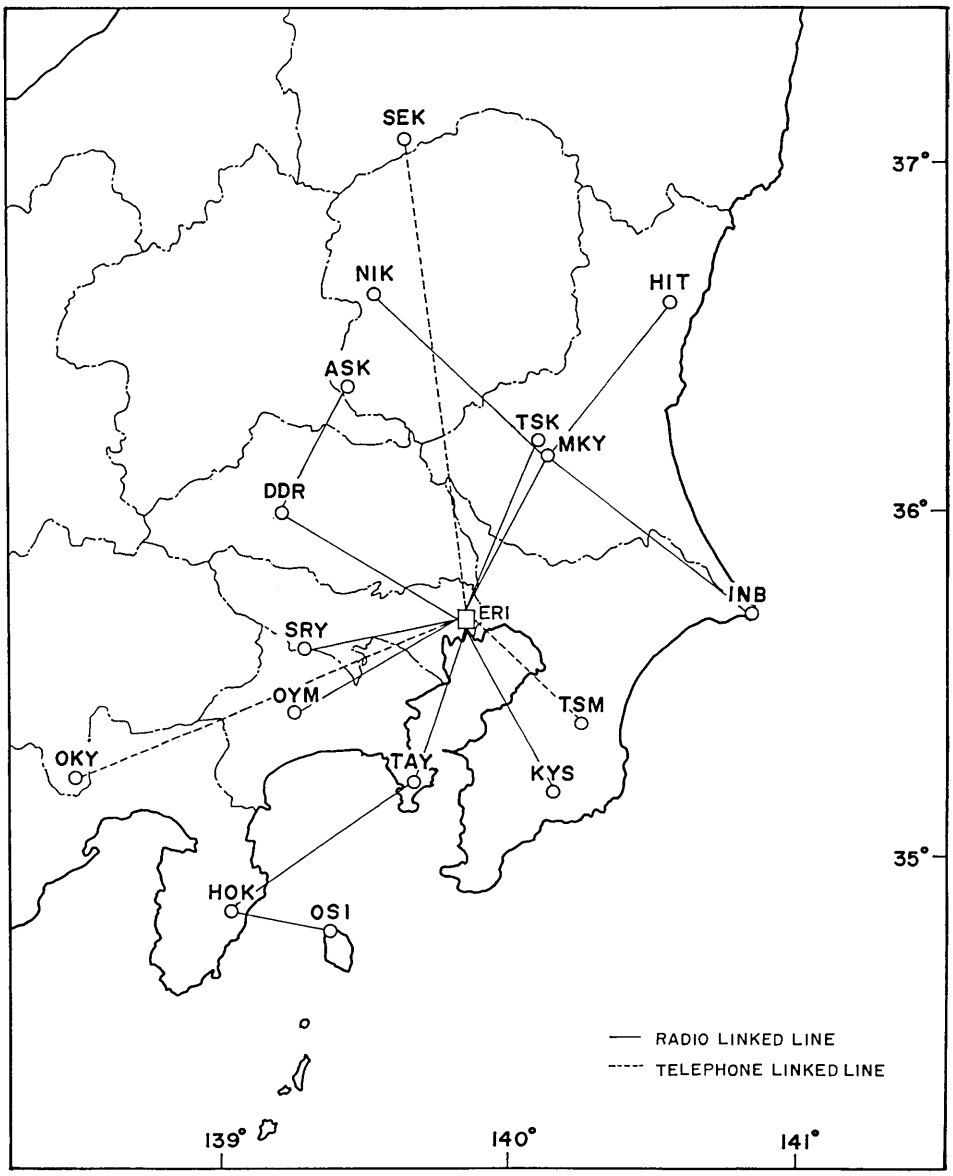

Fig. 3. Location of the permanent seismographic stations for microearihquake observation in the Kanto district operated by E. R. I.

which is equivalent to a capacity for transmitting 8 channeled seismic signals at a time. The NIK station is equipped with three component short period seismographs. Four channeled seismic wave signals, i. e., the three component high gain and one component low gain signals are continuously transmitted to the central station by a radio linked line. The

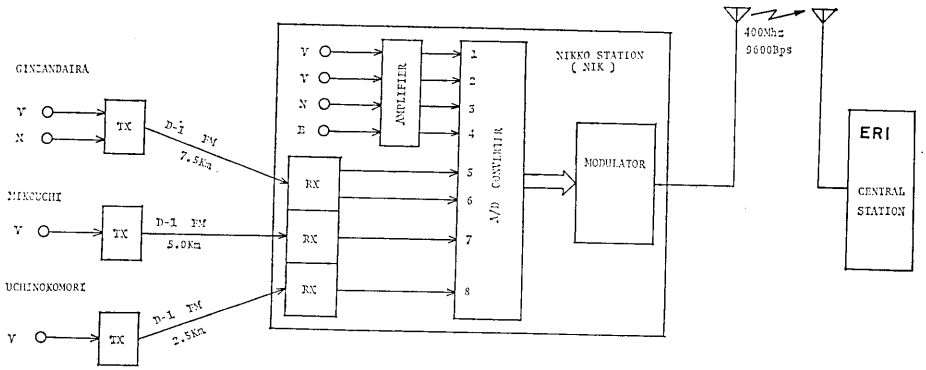

Fig. 4. Outline of the telemetering network system linking the temporary stations of Ginzandaira (GIN-1), Mukouchi (MKU) and Uchinokomori (UHK) with the central recieving station of E. R. I. in Tokyo through the permanent station NIK.

other four channels are left for temporary observations by setting up a local network in the area surrounding NIK. Both of the signals from NIK as well as from temporary stations can be recieved at the central station through the line from NIK.

A portable type of FM telemetering system has been developed to link the temporary stations with the key station NIK. A vertical component seismograph was installed at the Uchinokomori (UHK) and Mikouchi (MKU) stations and a vertical and horizontal component seismographs were installed at the Ginzandaira (GIN-1) station. The 8 channeled signals of the temporary network transmitted from NIK were fed into the automatic earthquake data processing system at the central station to detect and locate microearthquakes. The outline of the telemetering network system used for the present study is shown in Fig. 4.

The temporary local network covered the area of the earthquake swarm activity on the west bank of the Watarase river flowing along the western border of the Ashio mountain block. Though the network was relatively short spanned compared with the entire area of the swam activity on the border of Tochigi and Gunnma Prefectures, earthquakes with a M of larger than 1.5 in the area of about $20 \times 30\,\mathrm{km}^2$ near Ashio were located by the network with the error of less than 2 km.

3. Microearthquake distribution

No remarkable earthquakes with a M of more than 5.0 have been registered by J. M. A. (Japan Meteorological Agency) on the border of Tochigi and Gunma Prefectures except the Imaichi Earthquake of 1949 in the western part of the swarm area. Distribution of microearthquakes

in and around Tochigi Prefecture with focal depths of less than 50 km for the period from September 1980 to October 1981 is shown in Fig. 5 with an indication of the epicenter of the Imaichi Earthquake of 1949.

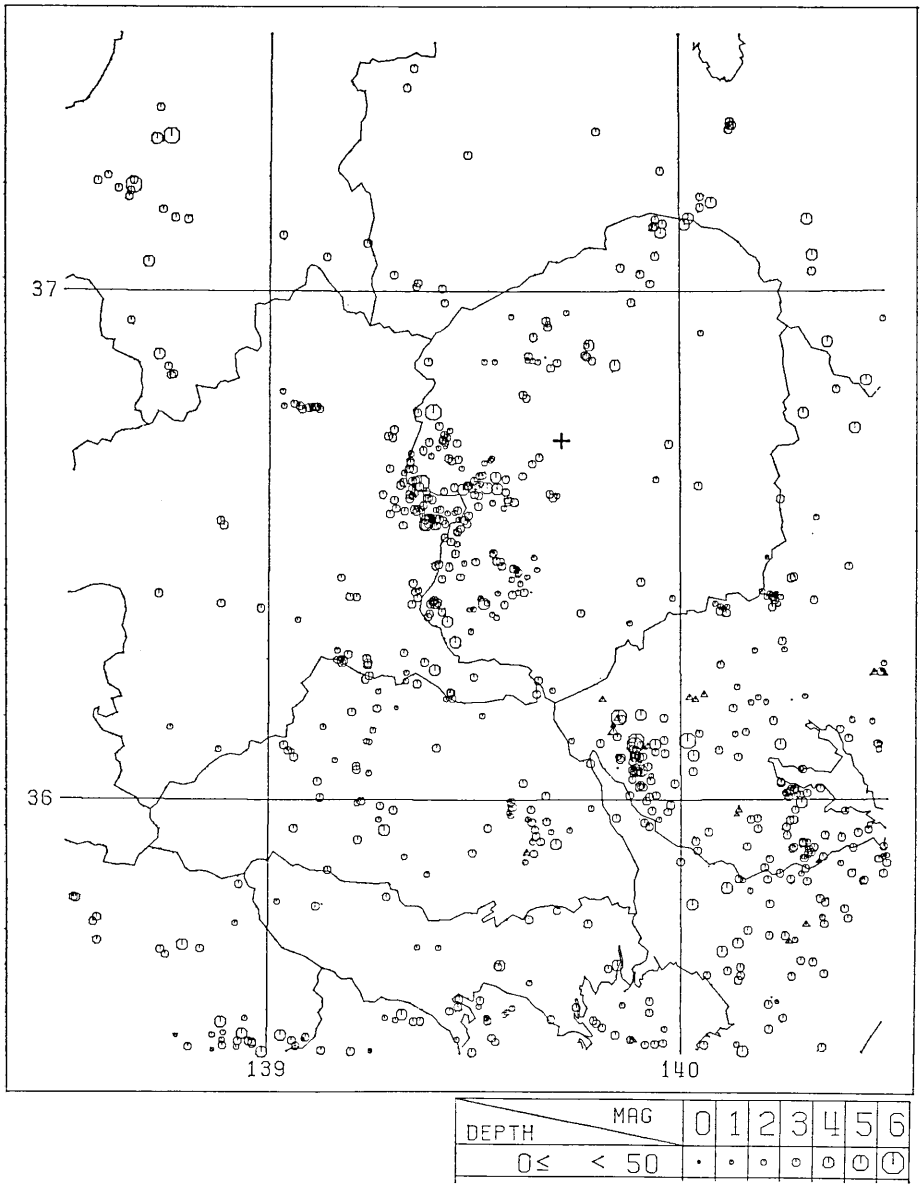

Fig. 5. Distribution of microearthquakes in and around Tochigi Prefecture with focal depths of less than 50 km for the period from September 1980 to October 1981 with an indication of the epicenter of the Imaichi Earthquake of 1949 (M 6.4, M 6.7) by a cross.

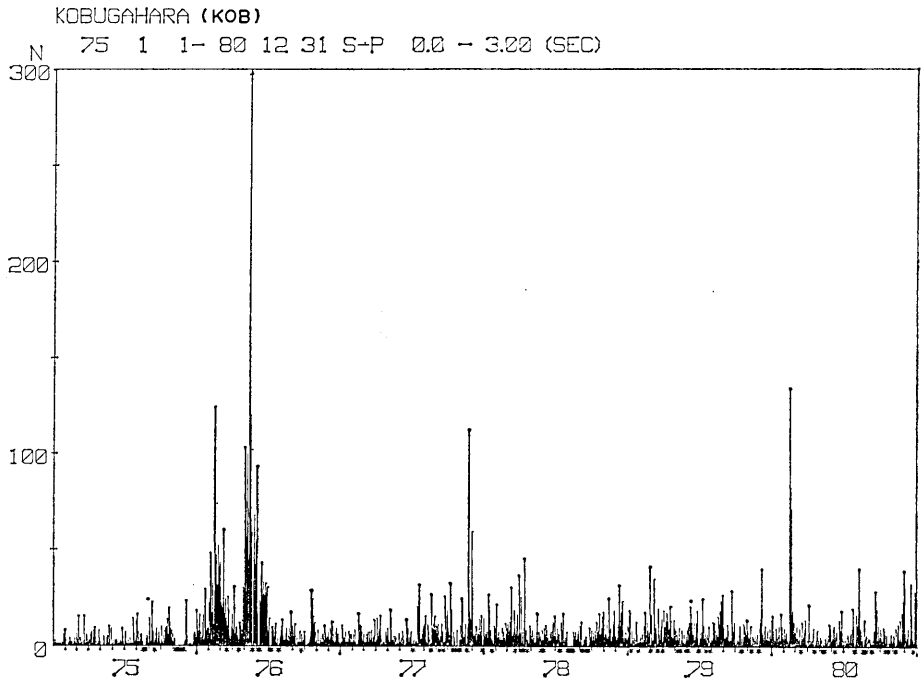

Fig. 6. Daily number of microearthquakes in the S minus P time of less than 3.0 sec at Kobugahara station (KOB). (after Karakama, personal communication)

A characteristic variation of the swarm activity with time in the Ashio mountain block has been continuously monitored at the Kobugahara station (KOB) by a helical drum record since January 1975. As shown in Fig. 6, the daily number of microearthquakes in the range of an S-P time of less than 3.0 sec at KOB is usually less than 20. When there was an occasional burst type of activity, the daily number of quakes became more than 100. The areal extension of the swarm activity was outlined by the routine network observation of microearthquakes in the Kanto district. With a distinct separation from surrounding activities, the swarm activity occupies the area of about $20 \times 30\,\mathrm{km}^2$. For routine observations, the stations are too sparsely distributed to study the detailed structure of seismicity within the swarm area. By means of a temporary tripartite network observation near Ashio from August 1972 to March 1973 (Fig. 10), a cluster of microearthquake epicenters was found along the east bank of the Watarase river flowing through the Ashio area trending in a NE-SW direction (OGINO, 1974). At each station, seismic signals were recorded by a short period vertical component seismograph on a helical drum recorder with a paper speed of 4 mm/sec. Hypocenters were cal-

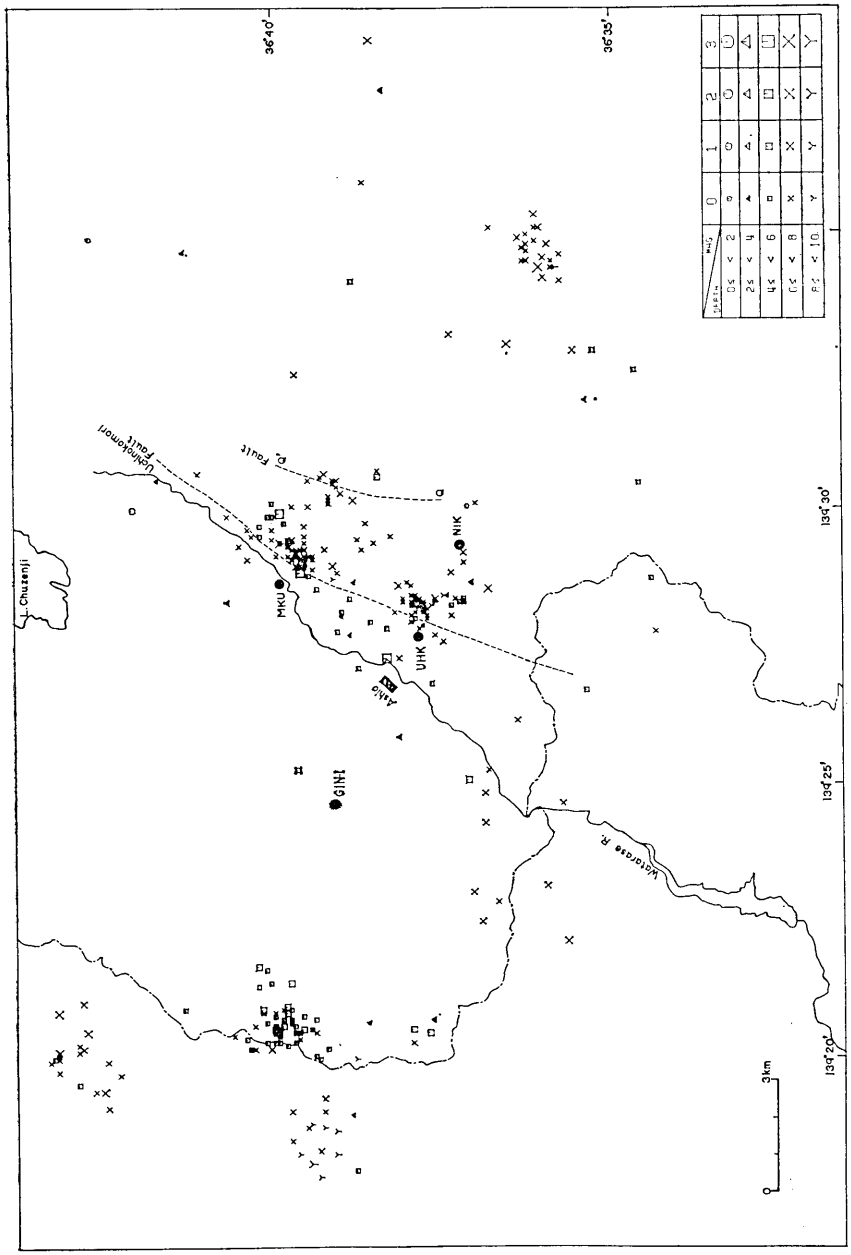

Fig. 7. Microearthquake distribution near Ashio obtained by the temporary observation network as shown in Fig. 2. Active faults are indicated by dashed lines.

culated by using the S minus P time instead of the P arrival time, because the standard time signals were missing for most of the events observed. Unclear onsets of S arrivals resulted in inaccurate S minus P times and, consequently, unreliable hypocentral determination.

In oder to make an extensive study on the reflections near Ashio with more accurate data, a telemetering network system was introduced as described in the previous section. Nearly 80 microearthquakes were located in the period from November 1981 to March 1982 as shown in Fig. 7. Several epicentral groups were detected by the hypocentral determination

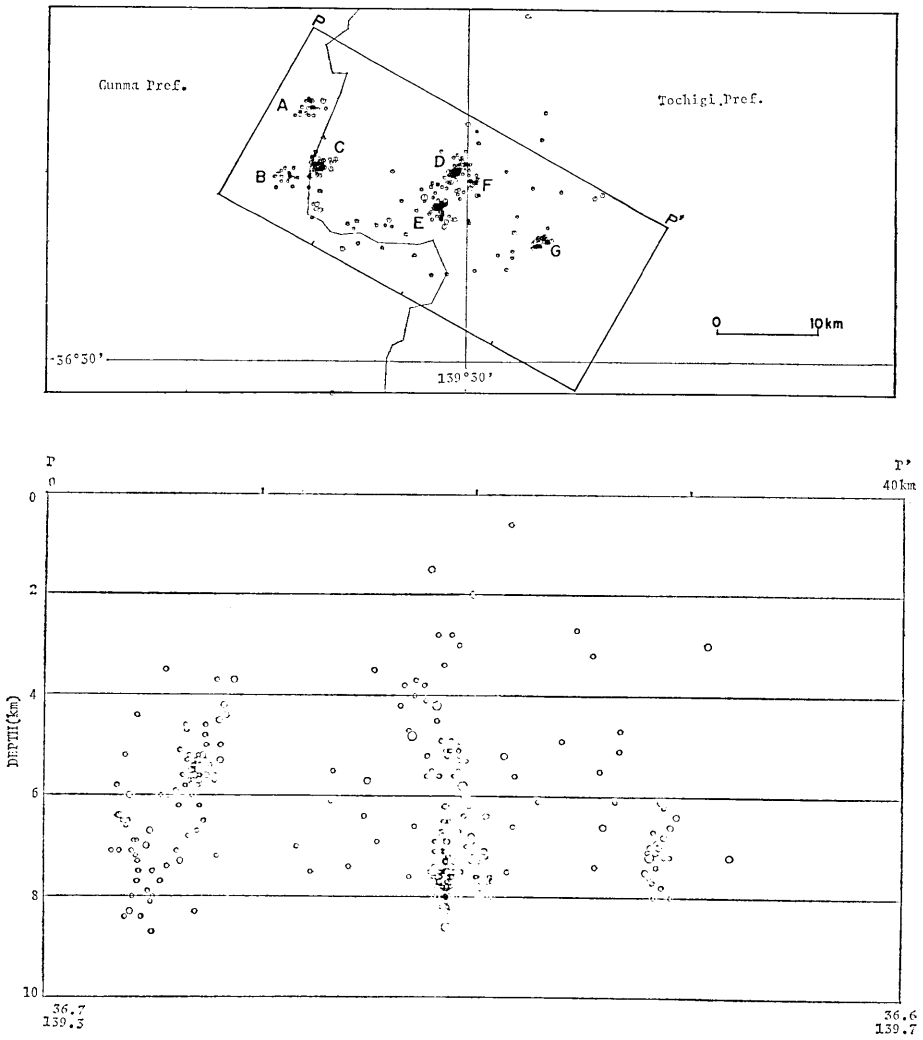

Fig. 8. Epicentral groups of A, ~, G (upper figure) and the corresponding vertical cross sectional profile ofhypocentral distribution (lower figure).

from the precise arrival times of the P and S waves obtained from the reproduced strip chart records with a paper speed of 20 mm/sec.

About 12 km west of Ashio, earthquake swarm activities were found in three separate areas of about 2×2 km^2 on the border of Tochigi and Gunma Prefectures as designated by A, B and C in Fig. 8. Along the east bank of the Watarase river, a remarkable swarm activity was found to have a linear alignment of epicentral distribution trending in a NNE-SSW direction with concentrated epicenters in the two small areas of D and E as shown in Fig. 8. The characteristic distribution of epicenters well agreed with the trace of the Uchinokomori fault in the Ashio mountain block (THE RESEARCH GROUP FOR ACTIVE FAULTS OF JAPAN, 1980). A composite fault plane solution for the earthquakes located in the fault zone was obtained by superimposing the data of the initial motion of the P waves of individual events. As shown in Fig. 9, the fault plane solution suggested a reverse type faulting with strike in the direction of about N28°E. When the upheaval of the western block of the fault relative to the eastern block is then assumed based on geological and geomorphological evidence (THE RESEARCH GROUP FOR ACTIVE FAULTS OF JAPAN, 1980), the dip of the fault should be taken as about 35°. In addition to the major pattern of seismic activity on the Uchinokomori fault, a minor epicentral group of F, as shown in Fig. 8, was found on the trace of the active fault QQ' in Fig. 7 running parallel to the Uchinokomori fault. About

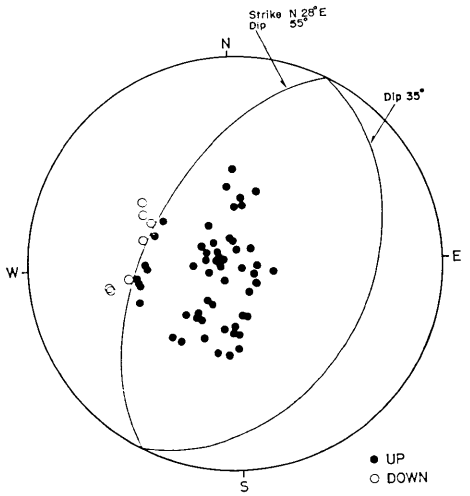

Fig. 9. Composite fault plane solution obtained from the P wave data of the microearthquakes located along the trace of the Uchinokomori fault (Equal area projection for the upper hemisphere).

10 km ESE of Ashio, a concentrated epicentral patch G was found to occupy the area with a diameter of less than 2 km.

A profile of the vertical cross section of earthquake distribution for the map in the upper figure of Fig. 8 is shown in the lower figure of Fig. 8. Though the focal depths have a considerable variation for each epicentral groups of A, ~G, they are not deeper than 8.5 km. The abrupt disappearance of seismic activity at the very shallow depth of 8.5 km may be related to some geophysical environment preventing the occurrence of earthquakes in the deeper parts of the earth's crust. It would be worth while to mention in this connection that the seismic activity near Ashio is one of the earthquake swarms in and around the geothermal or volcanic zones extending from northern Tochigi Prefecture to northern Fukushima Prefecture, as shown in Fig. 20 (SEIKA, 1973). An abnormally high temperature within the earth's crust in the volcanic zones may be a cause for the extremely shallow origin of the swarm activity near Ashio.

4. Characteristic features of the reflections of S_xP and S_xS

A preliminary travel time analysis of the crustal reflections in the

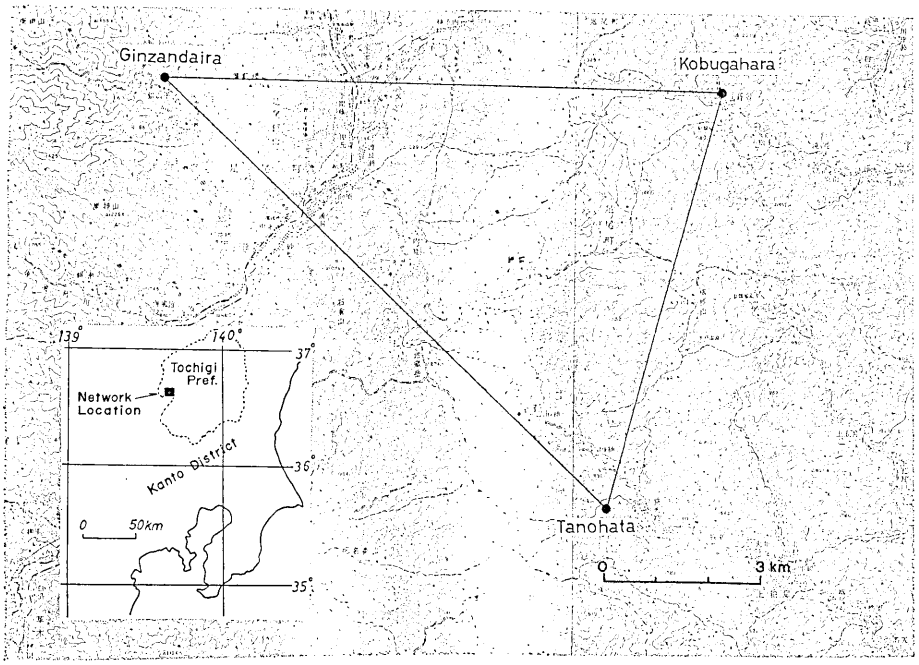

Fig. 10. Location of seismographic stations for temporary observations in the vicinity of Ashio, the northern Kanto district, operated in the period from August 1972 to March 1973 (after OGINO, 1974).

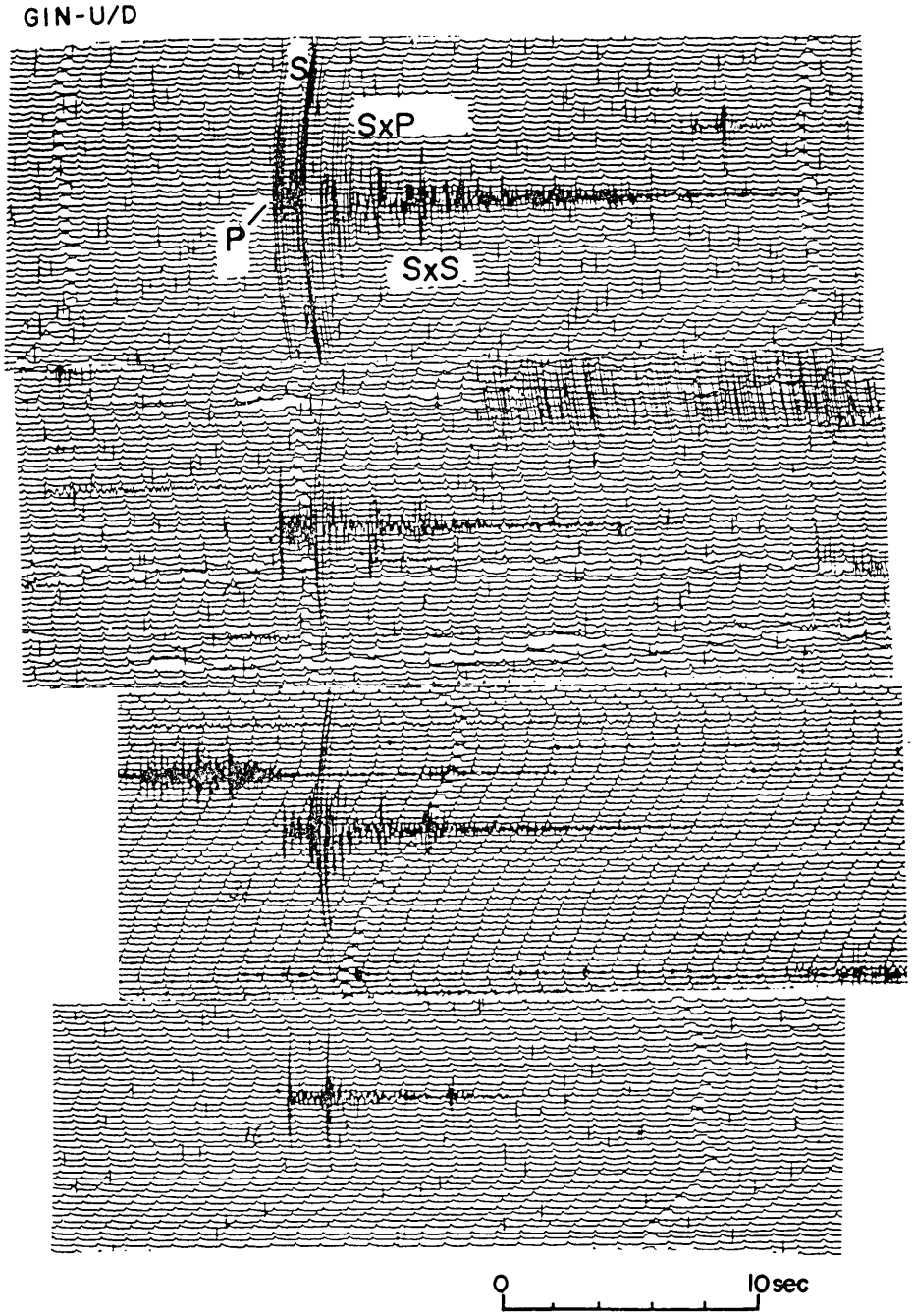

Fig. 11. Portions of helical drum seismograms for the vertical component at a paper speed of 4 mm/sec recorded at GIN. The reflections are designated as S_xP and S_xS.

area near Ashio was made based on the data obtained by the microearthquake observation at the three stations of GIN (Ginzandaira), TNH (Tanohata) and KOB (Kobugahara) from August 1972 to March 1973, as shown in Fig. 10 (OGINO, 1974; MIZOUE, 1980). At the station of GIN, two sharp phases following the direct S wave by 2.5-3.0 sec and 4.5-5.0 sec were registered on the helical drum record in the S minus P time range of 0.9-1.5 sec. Portions of the helical drum seismograms of microearthquakes at the station are shown in Fig. 11. The seismic wave phases of similar type were detected at the stations of TNH and KOB. Though more than 50 events were commonly observed by the three stations, less reliable data for the P arrival times was obtained from the observation mainly due to the instability of recieving condition of the standard time signals at each of the stations. Therefore, the arrival time difference for the specified phases relative to the P arrival times was used for the preliminary travel time analysis. The observed time distance relation of the later phases was well explained by the near vertical S to P wave (S_xP) and S to S wave (S_xS) reflections from a deep crustal discontinuity, the depth of which was in the range of 14-17 km.

For a more detailed study on the characteristic features of the reflections, a telemetering seismic network was introduced for temporary observation as described in the previous sections. Examples of the 7 channeled reproduced seismograms are shown in Fig. 12. The following points are noticeable characteristics of the reflections registered on the seismograms.

i) The arrival time difference between the two reflections of S_xP and S_xS depends strongly on the station locations. For example, the arrival time difference between S_xS and S_xP at NIK is about 0.3 sec larger than that at GIN-1. In the case of the near vertical reflections, the arrival time difference of the two reflections is directly related to the depth of the discontinuity. The resolution of the arrival time measurement on the reproduced seismograms with a paper speed of 20 mm/sec is about 0.02 sec when the noise level is normal. Therefore, it will be very promising that the depth of the discontinuity can be precisely determined from the arrival time difference of the two reflections.

ii) It is clearly shown that the S_xP reflection is predominant on the vertical and the S_xS reflection on the horizontal component seismograms, respectively. This well agrees with an interpretation that the former S_xP phase is identified as the P waves and the latter as the S waves with a nearly vertical incidence. An analysis of the particle motion of the reflections shown in Fig. 13 gives more direct presentation of the near

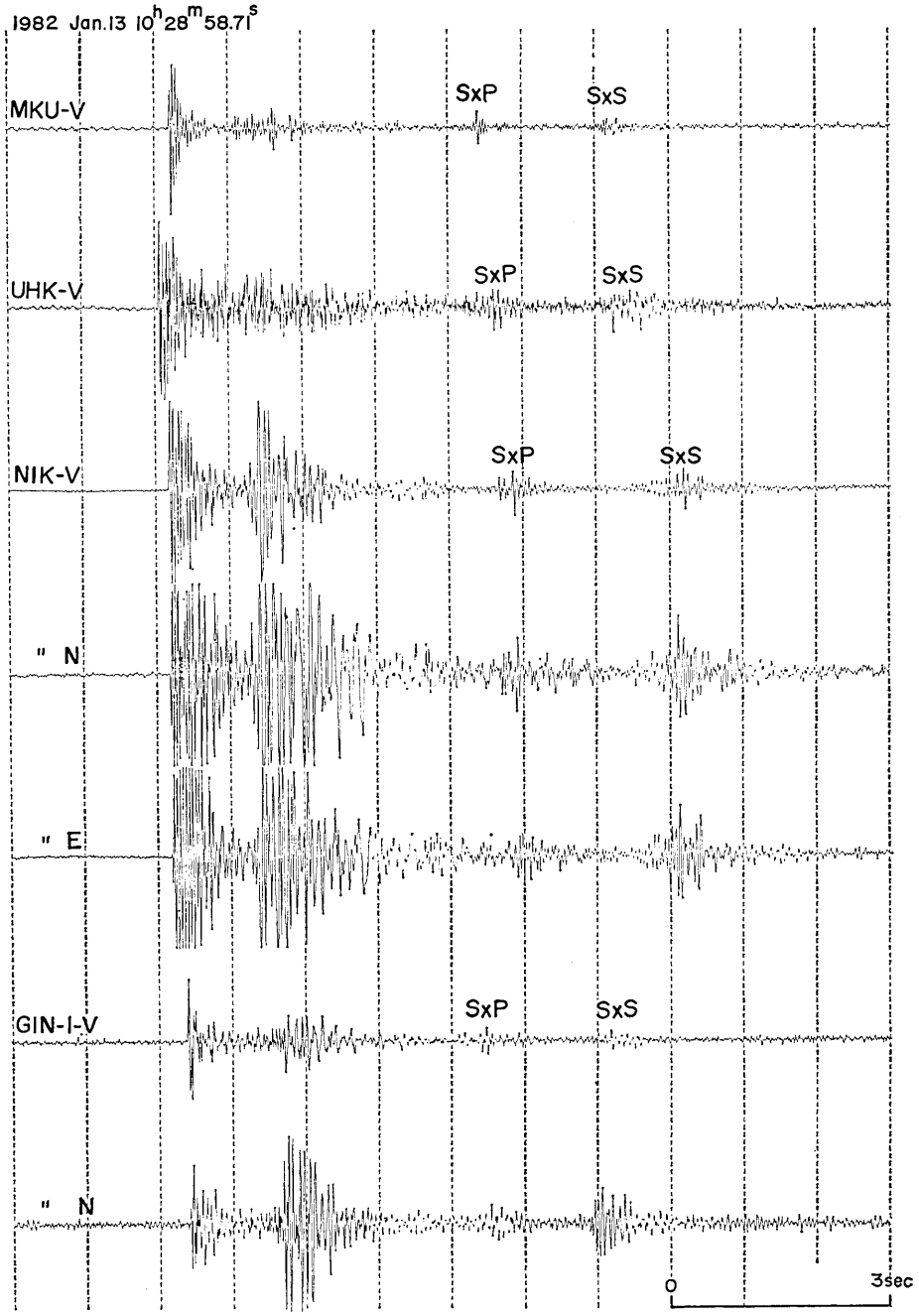
1982 Jan.13 10h28m58.71s
MKU-V
SxP
SxS
UHK-V
SxP
SxS
NIK-V
SxP
SxS
" N
" E
GIN-I-V
SxP
SxS
" N
0
3sec

Fig. 12a.

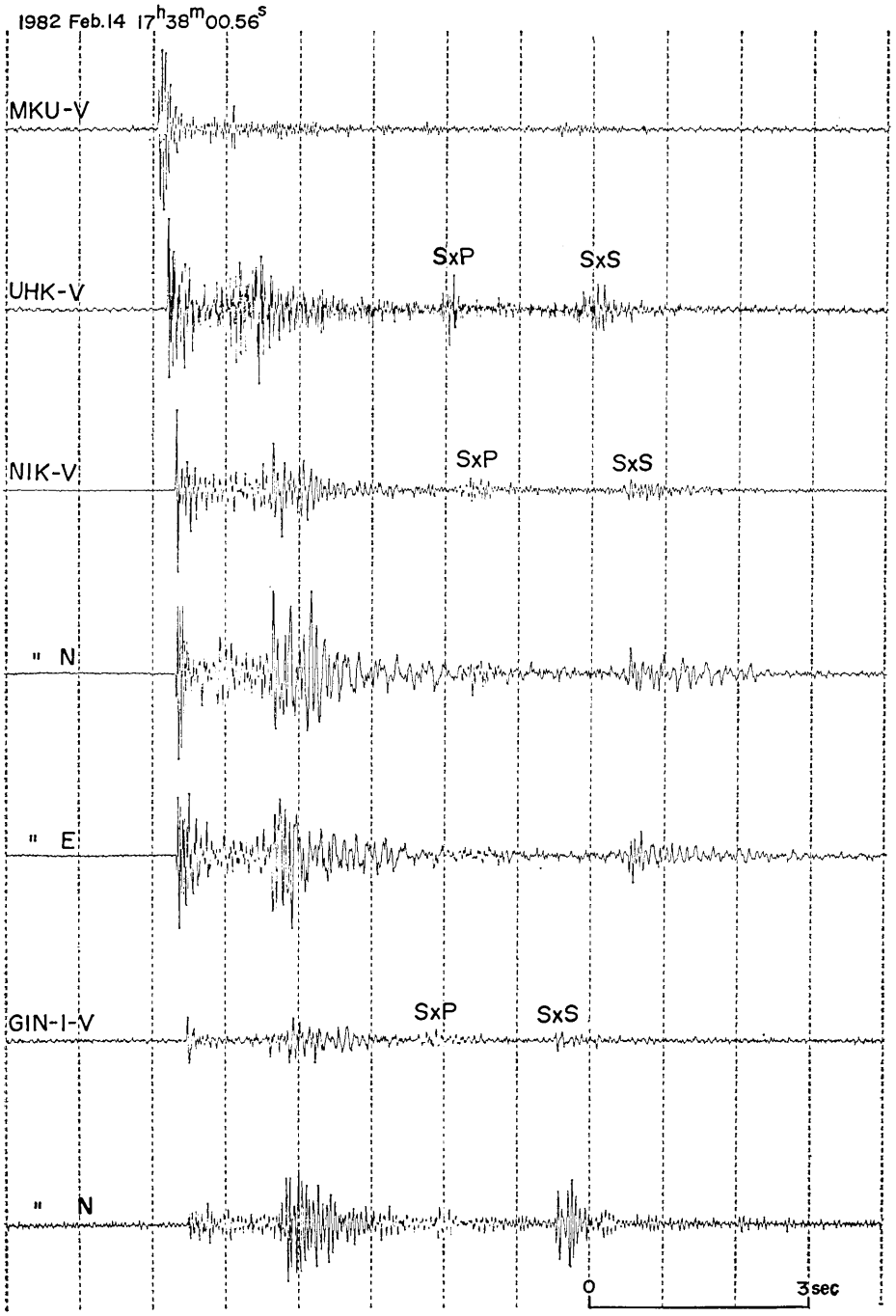
1982 Feb.14 17h38m00.56s
MKU-V
UHK-V
SxP
SxS
NIK-V
SxP
SxS
" N
" E
GIN-I-V
SxP
SxS
" N
0
3sec

Fig. 12b.

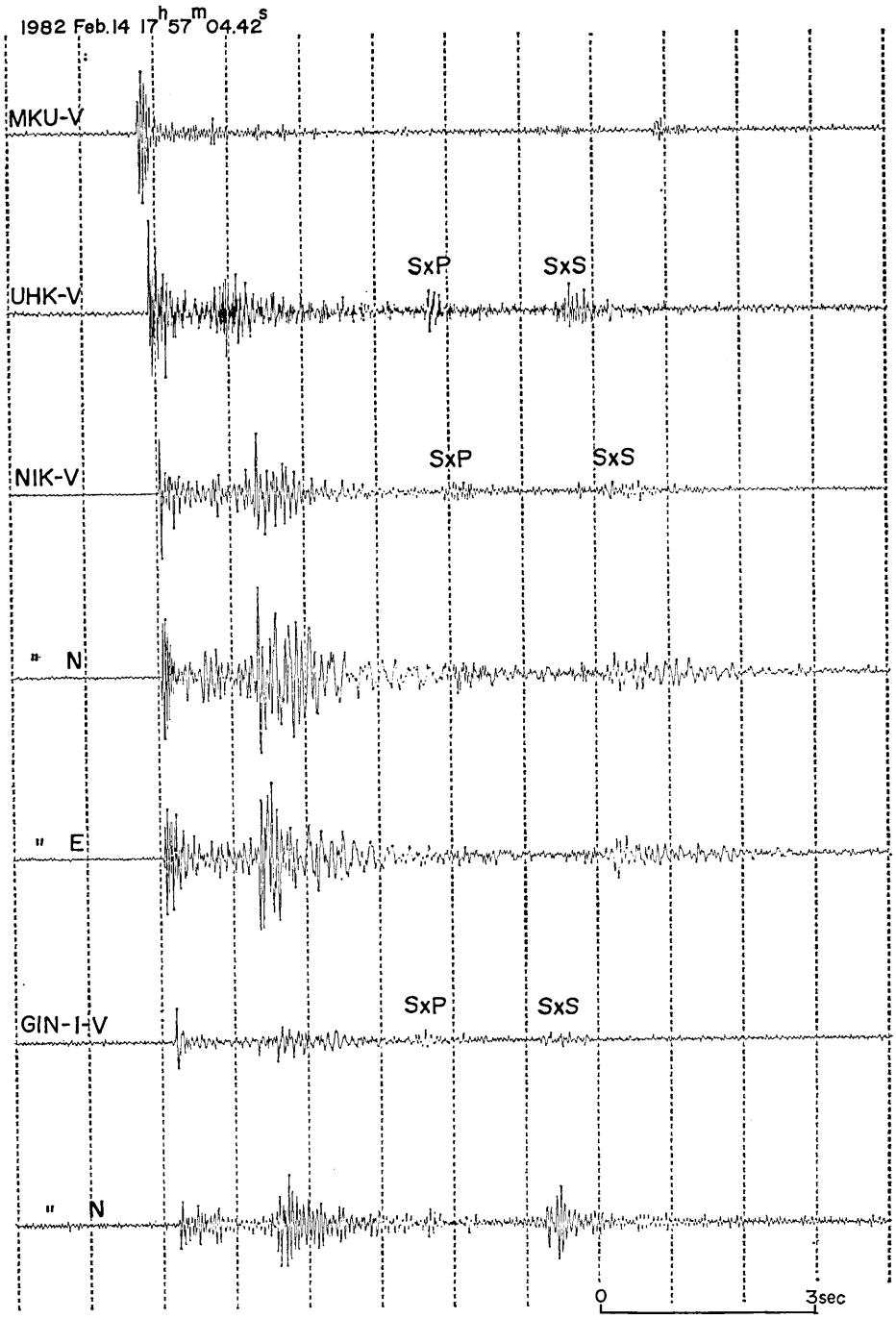
1982 Feb.14 17h57m04.42s
MKU-V
UHK-V
SxP
SxS
NIK-V
SxP
SxS
" N
" E
GIN-1-V
SxP
SxS
" N
0
3sec

Fig. 12c.

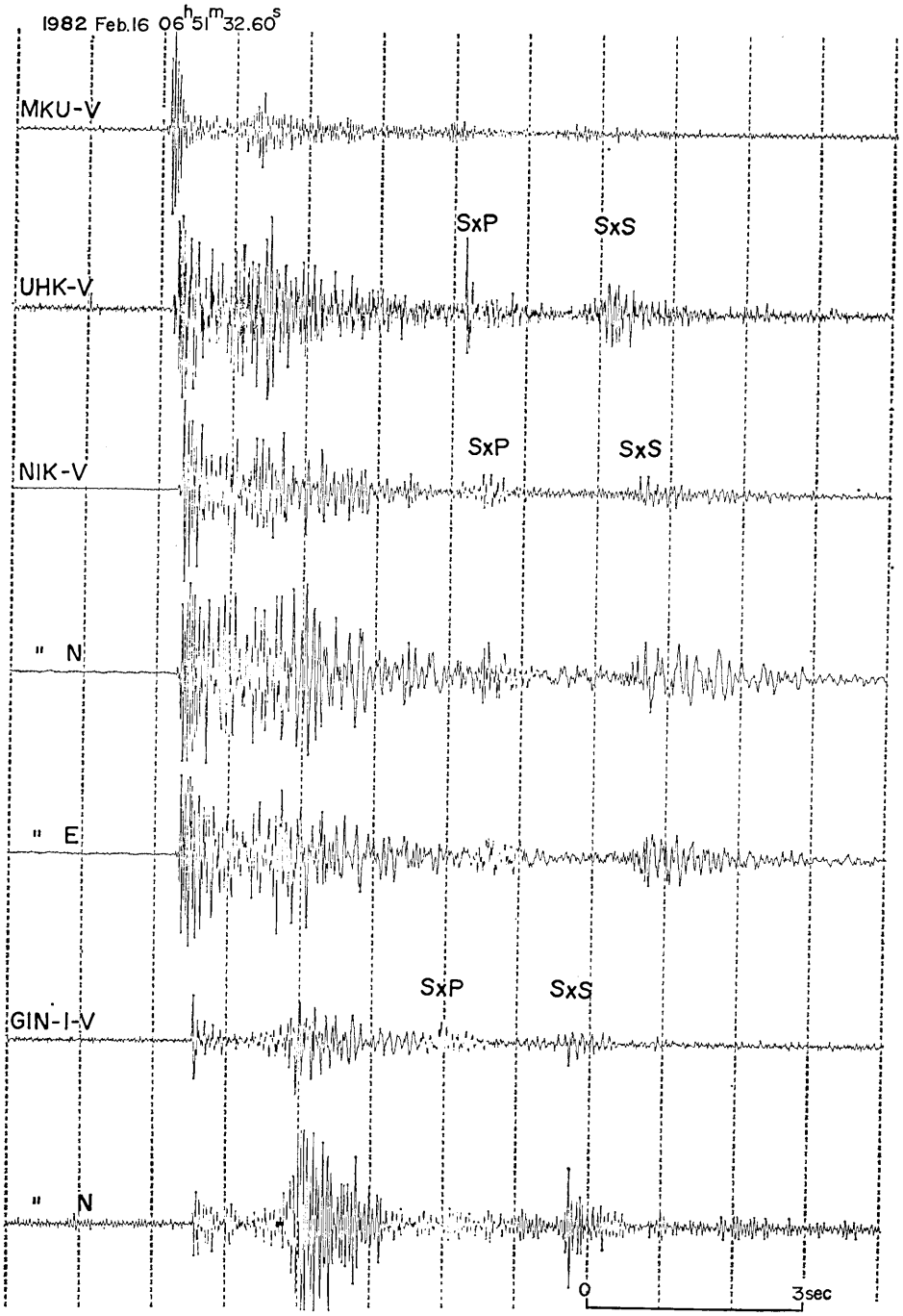
1982 Feb.16 06h51m32.60s
MKU-V
UHK-V
SxP
SxS
NIK-V
SxP
SxS
" N
" E
GIN-I-V
SxP
SxS
" N
0
3sec

Fig. 12d.

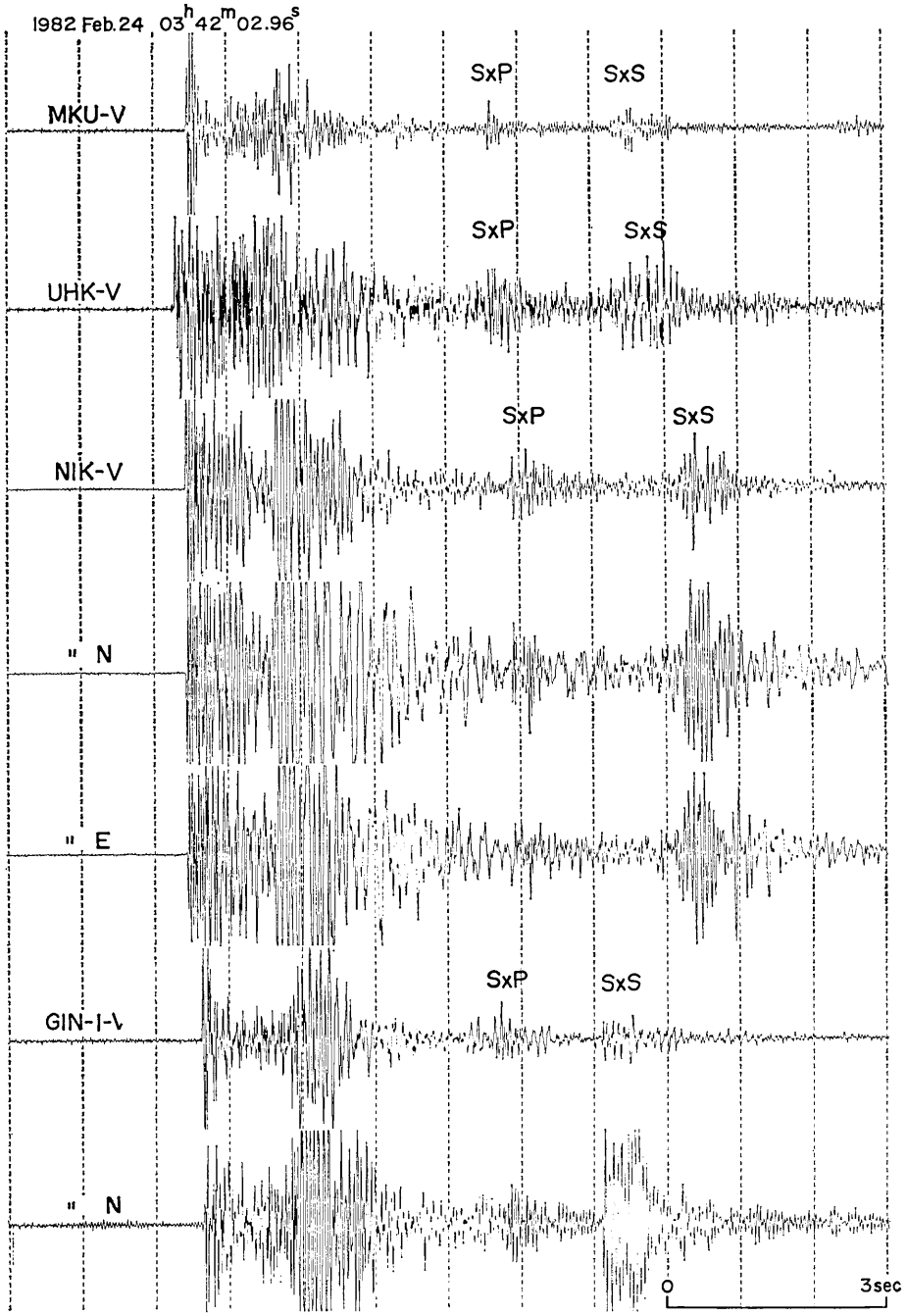

Fig. 12e.

Fig. 12. Multichanneled seismograms reproduced from digital magnetic tapes. Three components (vertical, NS and EW components) for NIK, two components (vertical and NS components) for GIN-1 and one component (vertical) of seismograms for UHN and MKU are shown. The reflection phases are indicated with designations of S_xP and S_xS.

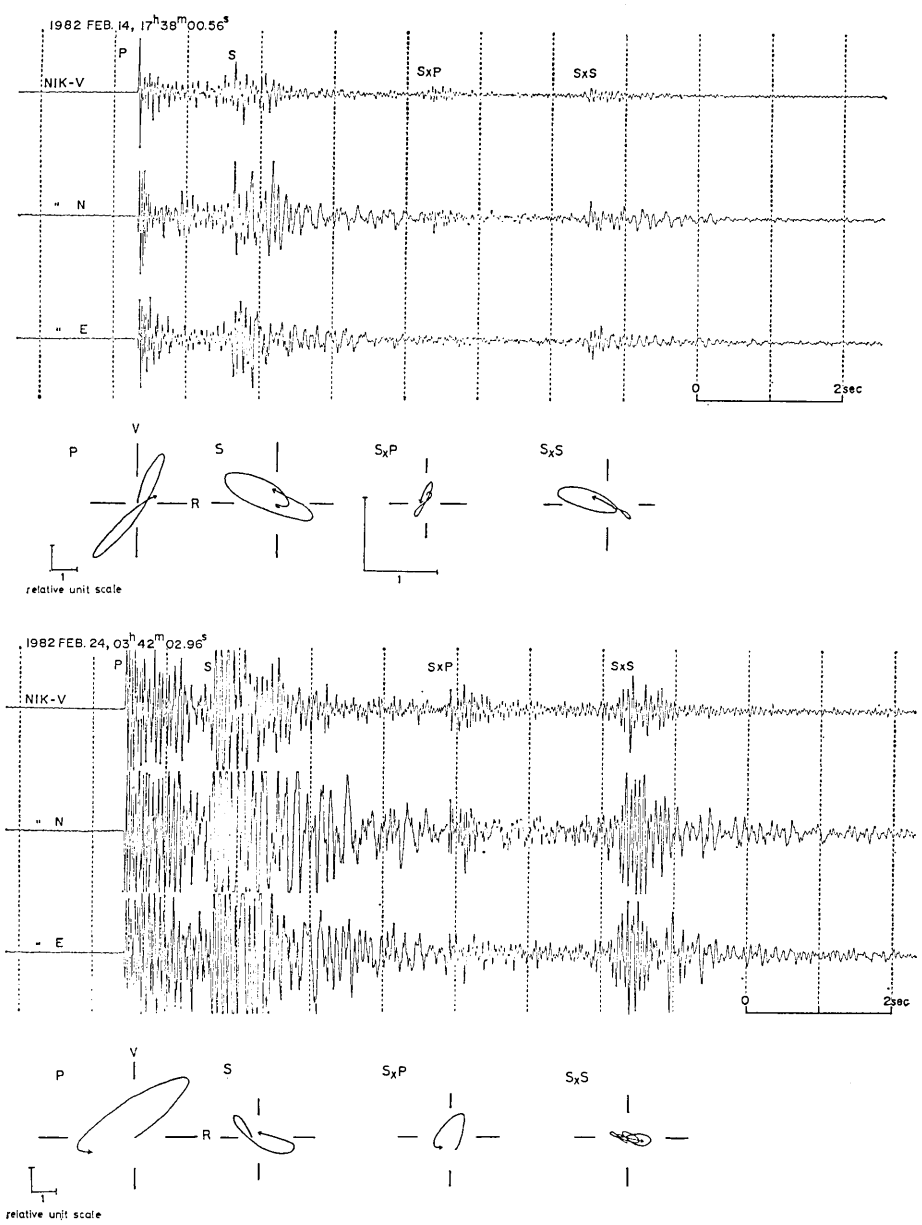

Fig. 13. Examples of time variations of particle motions of the reflections of S_xP and S_xS in the radial and vertical plane recorded at NIK for the event located in the north from the station.

vertical incidence of the two phases.

iii) On some of the seismograms, the amplitude is extraordinarily large compared to the amplitude of the direct S waves when the near vertical incidence of the S_xS is taken into consideration. In the large amplitude of S_xS, it is rather usual for the amplitude ratio of S_xP to S_xS to be in the range of 0.045–0.34. The large amplitude of S_xS suggests the existence of an unusual discontinuity with a large reflection coefficient for S to S-wave reflections.

iv) The reflections of S_xP and S_xS are not always strong enough to be recognized on the seismograms. The amplitude of the reflections seems to be related to the station location, hypocentral coordirates and the physical property of the discontinuity. The boundary of the areal extention of the unusual discontinuity will be given by examining the amplitude variation of the reflections over the extensive area of the earthquake swarms in the vicinity of Ashio.

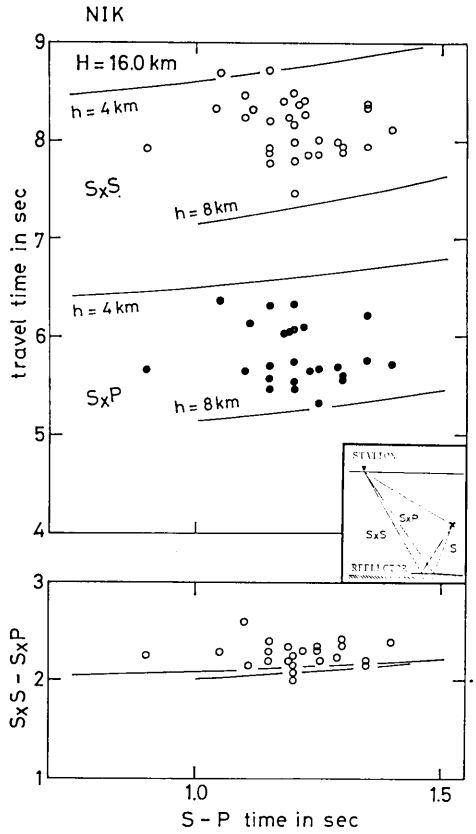

Fig. 14a.

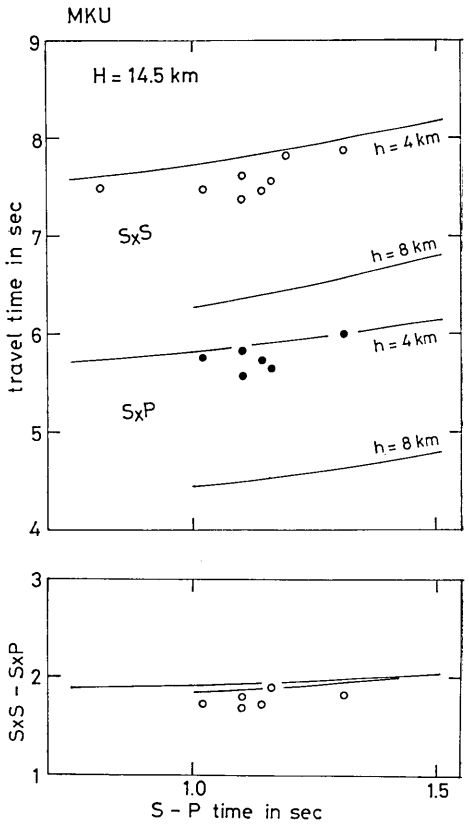

Fig. 14b.

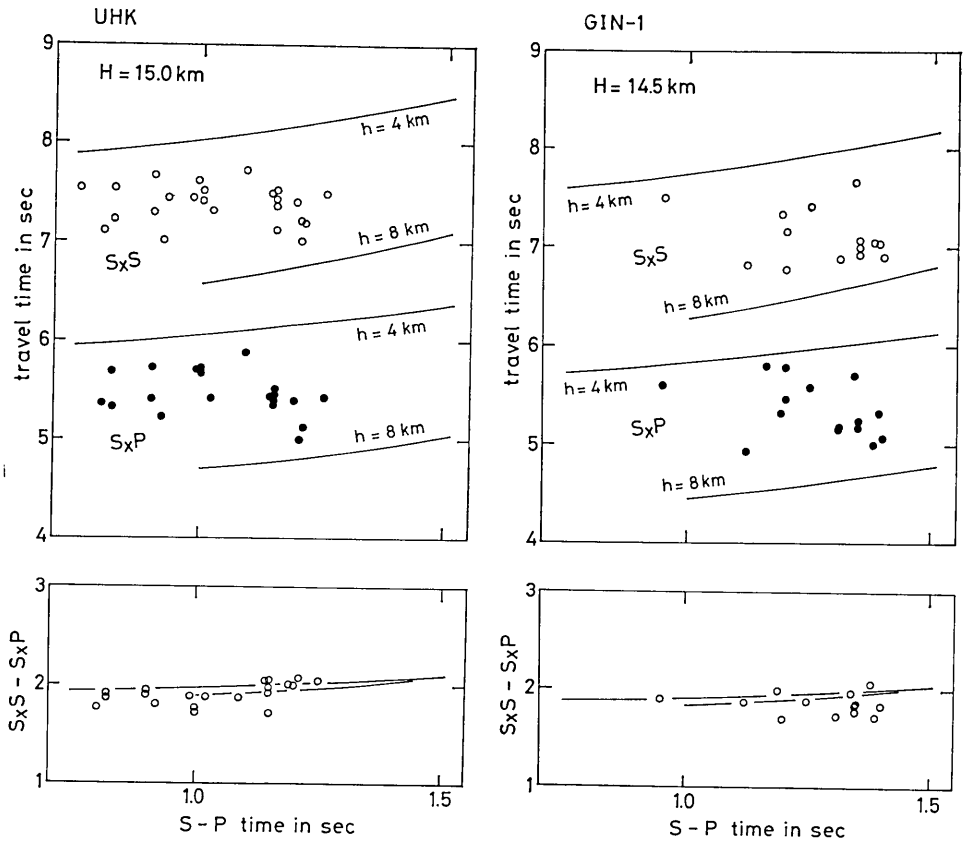

Fig. 14c. Fig. 14d.

Fig. 14. Observed and theoretical travel times of the reflections of S_xP and S_xS and the corresponding trval time difference of the two reflections versus S minus P time at the stations of NIK, MKU, UHK and GIN-1. Inset shows the ray paths of S_xP and S_xS. Two curves for the reflections from the depth H (solid lines) in given, one for the minimum, the other for the maximum depth of focus h.

5. Mapping of the unusual discontinuity

Time distance relations of the reflections of S_xP and S_xS were studied for the stations NIK, GIN-1, UHK and MKU. The travel times of the reflections are plotted on the graphs in Fig. 14, which covers the S minus P time of less than 1.5 sec. Theoretical travel time curves for the reflections from a depth H are also drawn in Fig. 14 for each of the stations with a best fit to the observational data. Two curves for the reflections are given, one for the minimum, the other for the maximum depth of focus h. The left hand side ends of each curve are the theoretical limit of observable reflections at the specified depth of focus. As a result

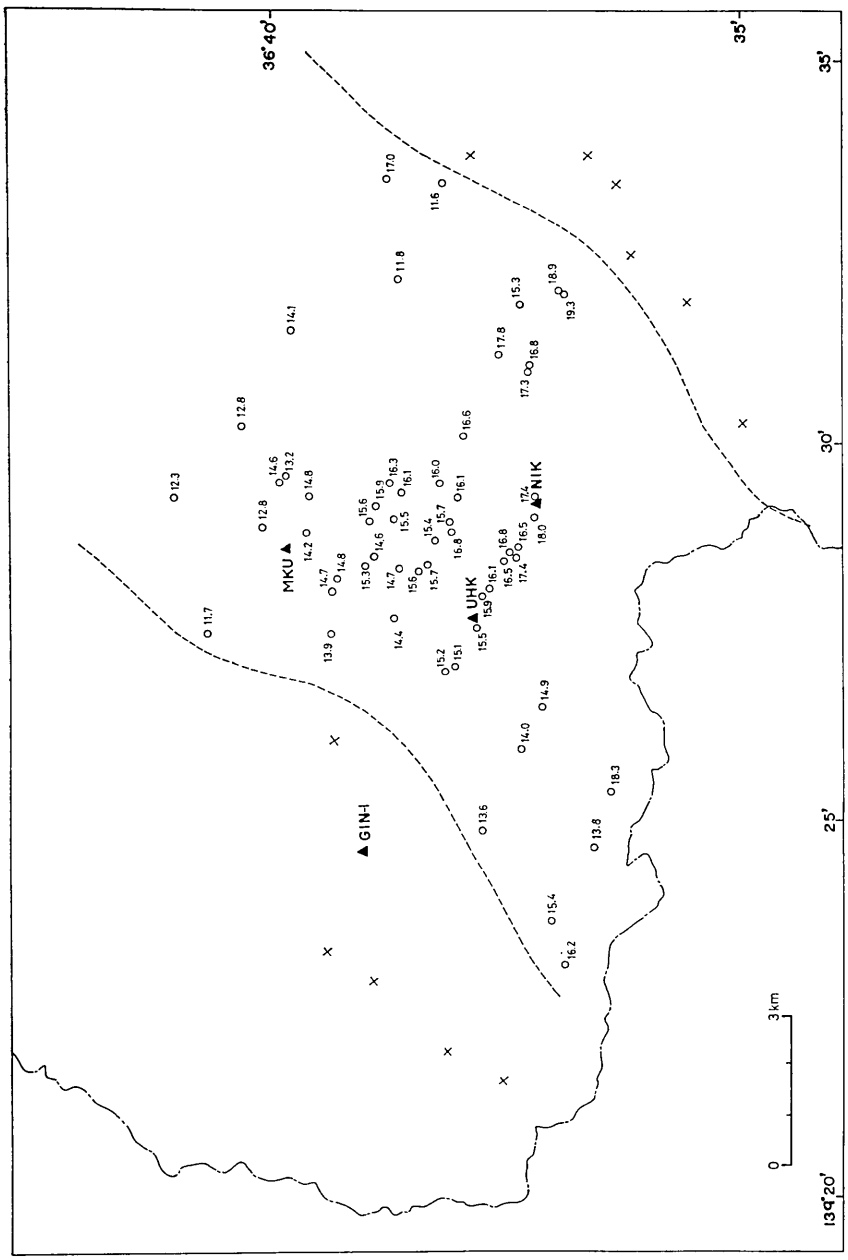

Fig. 15. Map showing the depth of reflection points (open circles) in kilometers. Boundaries of the zones in which strong or moderate reflections were observed are indicated by dashed lines.

of the time distance relations, the depths of the discontinuity beneath the stations of GIN-1, MKU, UHK and NIK were found to be about 14.5, 14.5, 15.0 and 16.0 km, respectively. In the above procedure of the travel time analysis, the P wave velocity of V_p 5.8 km/sec and the S wave velocity of V_s 3.35 km/sec were given as represented by the theoretical travel time curves in Fig. 14. In general, only one combination of the focal depth h and the depth of the discontinuity H will produce the theoretical curves that fit the observed data of the reflections of S_xP and S_xS equally well. In such a particular case, the theoretical travel time curves bracket both S_xP and S_xS data in about the same way, so that little adjustment in the value of H, h, V_p and V_s is possible. The seismic wave velocities of V_p and V_s were assumed to be constant from the earth's surface to the depth of the discontinuity.

In order to evaluate the depth of the discontinuity, 20 earthquakes

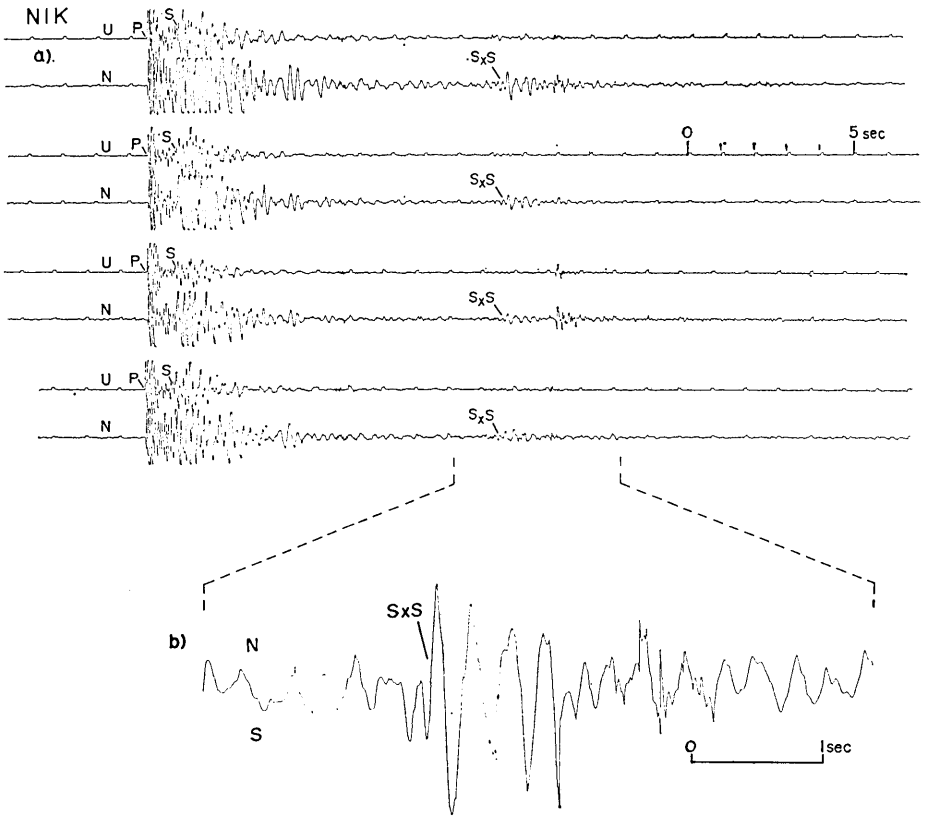

Fig. 16. Original (a) and enhanced (b) seismograms of the reflections S_xS generated by the quarry blasts at a site near NIK.

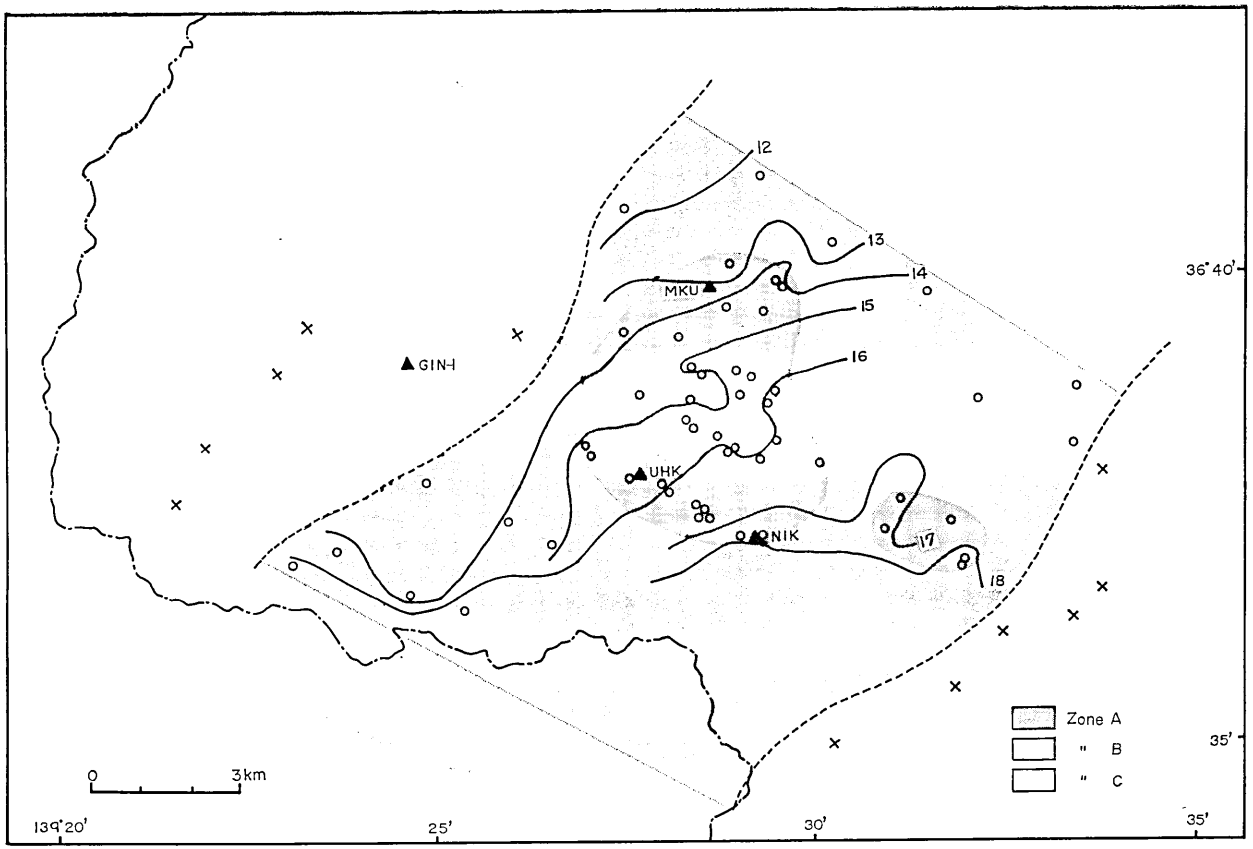

Fig. 17. The hatched zones correspond to the reflection points of strong (Zone A) and moderate (Zone B) modes of reflections. Outside of the hatched zones (Zone C), no reflections were detected. Hypothetical reflection points from which no reflections were observed are indicated by crosses. The locations of seismographic stations used are shown by solid triangles.

located with the highest accuracy were selected. Reflection points were given for these earthquakes by using good quality data of S_xS travel times in combination with the hypocentral coordinates. A total of 54 reflection points were plotted on the map in Fig. 15. In the evaluation of the depth of the reflection points, the discontinuity was tentatively assumed to be horizontally layered at each reflection point. The calculated depths at the individual reflection points were indicated in Fig. 15. A systematic depth change of the reflection points was found by the analysis as shown by the contour lines of a 1 km depth interval in Fig. 17. The discontinuity was found to be inclining in the direction of about S25°E with considerable local irregularities. The large variation in the depth of the discontinuity within a small area suggests an unusual nature of the discontinuity, though the result shown in Fig. 17 may partly be affect by an inaccurate estimation of the depth of the individual reflection points. The vertical cross sectional profile of the unusual discontinuity in relation to the microearthquake distribution projected on PP′ in Fig. 8 is illustrated in Fig. 18.

Quarry blasts at a site several kilometers from NIK were found to

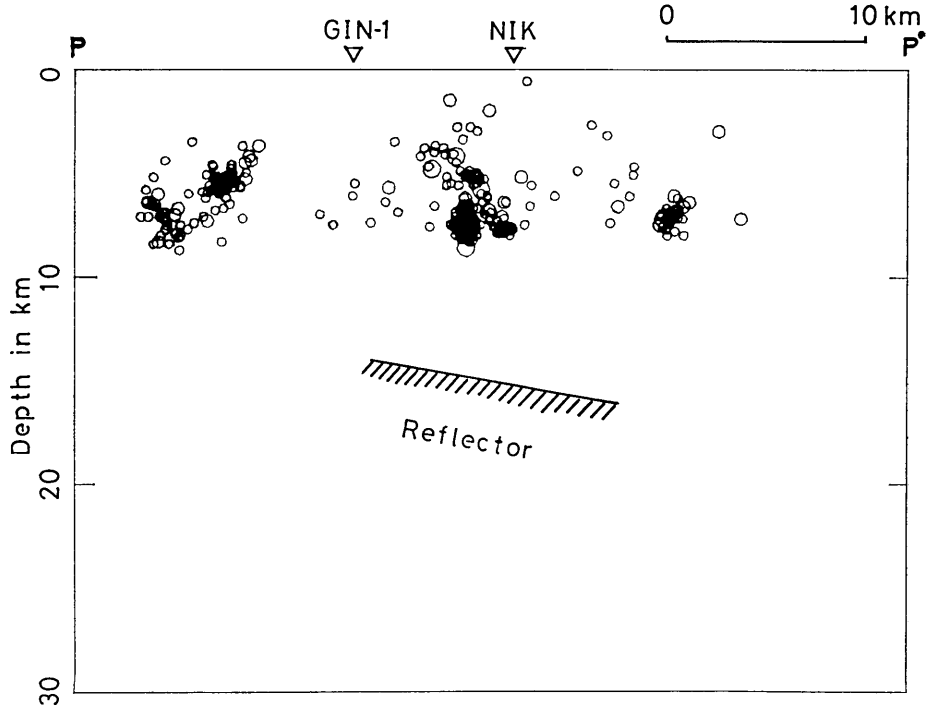

Fig. 18. The vertical cross sectional profile of the unusual discontinuity in relation to the microearthquake distribution projected on PP′ in Fig. 8.

produce strong S_xS reflections on the horizontal component seismograms at NIK, as shown in Fig. 16-a. A simple summation of the waveform data of the reflections from the quarry blasts at the same shot site near NIK produced an enhanced signal for the reflection of S_xS, as illustrated in Fig. 16-b. The travel time of the reflection was given very precisely due to the improvement of a signal to noise ratio. The depth of the discontinuity beneath NIK obtained from microearthquake data was calibrated by the enhanced signal of the reflection from the quarry blasts, for which the shot point was precisely known. The depths of the discontinuity from different sources with nearly the same reflection point agreed within the limit of errors of about ± 0.5 km.

As shown in Fig. 17, a systematic zonal arrangement was given when the reflection points were classified by the spatial variation in the amplitudes of the reflections. Very strong reflections of S_xP and S_xS on both vertical and horizontal component seismograms were related to the reflection points in the first zone (Zone A) as shown in Fig. 17. The fairly strong S_xS, on horizontal component seismograms, were related to the reflection points in the second zone (Zone B). No clear reflections were detected from the points in the third zone (Zone C) outiside the first and the second zones. The area of the unusual discontinuity would not, therefore, be extended beyond the boundary of the second zone in Fig. 17 as bounded by two parallel lines aparting at a distance of about 10 km. Judging from the general trend of the hatched zone in Fig. 17, it seems to be probable that a horizontal extension of the unusual discontinuity strikes in a NE-SW direction along the general trend of the volcanic front in the area as shown in Fig. 20.

6. Properties of the discontinuity

It can be noticed that observations of crustal reflections at very small distances are quite rare. There were a few cases where near vertical S to S wave reflections from the Conrad discontinuity were registered on horizontal component seismograms of microearthquakes (MIZOUE, 1971; TSUKUDA, 1976). In the area near Ashio, the near vertical S to S wave reflections (S_xS) from the discontinuity at the depth of 14–17 km were characterized by large amplitude signals on both vertical and horizontal component seismograms with comparatively high frequency oscillations as shown in Fig. 12. When the amplitude of S_xS is comparable to that of S_xP on verical component seismograms, the S_xS energy apparently predominates the S_xP energy for a small angle of incidence. The large

amplitude of S_xS generally observed near Ashio suggests a substantial difference in S wave velocity across the discontinuity.

The velocity contrast across the discontinuity can be estimated by using the ratio of P_xS to S_xS amplitudes as a function of distance or incident angle if the plane wave reflection theory is applicable. The amplitude ratio of S_xP to S_xS will be little affected by differences in radiated energy from the focus, because S_xP and S_xS are generated by S wave energy traveling slightly separated ray paths from the focus. The theoretical reflection coefficient in relation to incident angles for S_xP and S_xS are presented in Fig. 19 for the crustal models of Model A and B as given in Table 1. Model A represents a normal crust, while Model B represents an unusual crust with a discontinuity underlain by a molten material. The observed amplitude ratios of S_xP to S_xS were obtained by averaging many observed ratios narrowly grouped about the angles of incidence as shwon in Table 2. The data for these ratios was obtained from vertical component seismograms at NIK. The measured amplitude ratios have been corrected by multiplying by the sine of the angle of

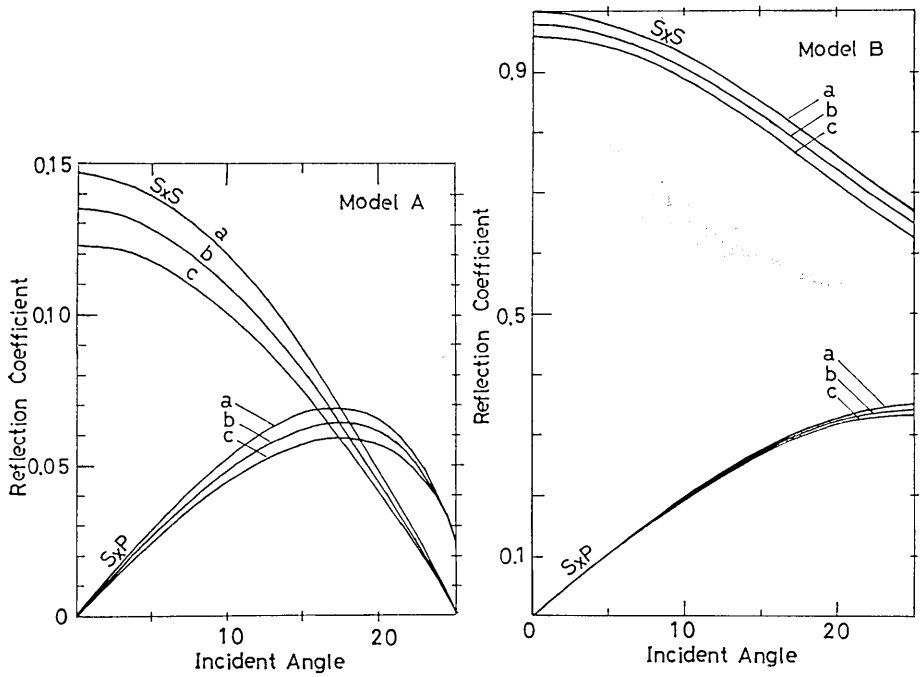

Fig. 19. Reflection coefficient of of S_xP and S_xS in relation to incident angles calculated for the unusual discontinuities underlain by a molten material (Model B) and for models with the Conrad discontinuity (Model A).

Table 1. Velocity models of the earth's crust used for the evaluation of the reflection coefficient of S_xP and S_xS phases.

	Model—A			Model—B		
	a	b	c	a	b	c
α_1	5.80	5.80	5.80	5.80	5.80	5.80
β_1	3.35	3.35	3.35	3.35	3.35	3.35
α_2	7.00	6.90	6.80	5.80	5.80	5.80
β_2	4.05	3.99	3.93	0.00	0.03	0.17
ρ_2/ρ_1	1.11	1.10	1.09	1.00	1.00	1.00

α_1, α_2; P wave velocities (km/sec) in the upper and lower layers.
β_1, β_2; S wave volocities (km/sec) in the upper and lower layers.
ρ_1, ρ_2; Densities in the upper and lower layers.

Table 2. Observed and theoretical ratios of S_xP to S_xS amplitudes for the crustal structures of Model A-a and B-b.

Observed				Theoretical Amplitude Ratio (S_xP/S_xS)	
Incident Angle		Amplitude Ratio (S_xP/S_xS)			
S_xP	S_xS	Measured	Corrected	Model A-a	Model B-a
2.1	3.1	0.84	0.045	0.091	0.045
6.2	9.7	0.91	0.15	0.29	0.14
8.4	13.7	0.94	0.23	0.46	0.19
11.5	18.3	1.00	0.33	0.93	0.29
15.8	22.8	0.76	0.34	1.36	0.35

incidence for the S_xS wave and dividing by the cosine of the angle of incidence for S_xP following the method as described by SANFORD et al. (1973). Theoretical amplitude ratios of S_xP to S_xS based on plane wave theory are presentated in Table 2 for the same angle of incidence as the observed ratios. The depth of the discontinuity is assumed to be 15.0 km based on the result in Figs. 15 and 17. For the S wave velocity contrast across the discontinuity from 3.35 km/sec to 4.05 km/sec for the Model A-a in Table 1, the theoretical amplitude ratios are greatly different from the observed ratios, particularly for the angle of incidence for S_xS of more than 10°. Assuming a discontinuity across which the S wave velocity decreases from 3.35 km/sec to 0.00~0.17 km/sec with depth while the P wave velocity remains the same as is for the Model B in Table 1, the discrepancy between the observed and theoretical values is greatly reduced. In addition, the steady increase in the observed ratios with increase in

the angle of incidence is duplicated with this type of discontinuity. The same tendency in the relation between the amplitude ratios and incident angle was found in the Rio Grande rift where an extensive sill shaped magma body has been confirmed (SANFORD et al., 1973).

From the above consideration, it can be concluded that the discontinuity beneath the earthquake swarm area near Ashio is underlain by low rigidity material having a P wave velocity little different from the overlaying material. A comparison of the characteristic features of the reflections observed near Ashio with those in the Rio Grande rift leads to a conclusion that the reflections in the two different regions are nearly identical not only in their general wave forms but also in their amplitude ratios for the incident angle of $0\sim23°$.

7. Discussions and conlusions

In the vicinity of Ashio in the northwestern part of Tochigi Prefecture, the northern Kanto district, very shallow earthquake swarms have been detected by microearthquake observations for surveillance of local seismicity. A temporary seismic network consisting of four telemetering stations equipped with high magnification short period seismographs was set up to make extensive studies of microearthquake distributions and crustal structures. The results obtained from the analysis of the observational data are summarized as follows.

i) The spatial distribution of microearthquakes related to the earthquake swarms has a characteristic fine structure with several patches of epicentral groups. Extremely shallow focal depths of less than 8.5 km characterizes the earthquake swarms. A prominent lineament of epicenters in the Ashio mountain block can be correlated with the Uchinokomori fault, one of the major active faults in the area. A composite fault plane solution for the microearthquakes occurring on the trace of the fault indicates the reverse type faulting with the strike of N28°E and the dip angles of 35° and 55° for the nodal planes.

ii) Microearthquake seismograms recorded by the stations near Ashio frequently have two sharp impulsive phases following the direct S wave. These phases were identified as S_xP and S_xS reflections from a sharp discontinuity at depths of 14–17 km.

iii) The depths of the reflection points for S_xS were obtained in the area near Ashio by using the travel times of S_xS in combination with a high precision hypocentral coordinates. A contour line map of the depth distribution of the discontinuity shows a general inclination dipping in a

SE direction with an abnormally large angle of 30-35°. The areal extension of the discontinuity related with the strong reflections seems to be restricted within a limited part of the area of the swarm activities.

iv) Observed values of the amplitude ratio A_{SxP}/A_{SxS} of the reflections S_xP and S_xS vary from 0.045 to 0.34 for the incident angle in the range from 0 to 23°. Considering that S_xP and S_xS are genrated by S wave energy traveling slightly separated ray paths from the focus, their amplitude ratio is relatively unaffected by differences in radiated energy from the focus (SANFORD et al., 1973). Therefore, the difference in the observed amplitude ratio can be attributed to the unusual physical properties of the discontinuity. Theoretical amplitude ratios based on the plane-wave theory were calculated by assuming various velocity models of the earth's crust. Fairly good agreement between theoretical and observed values was obtained when P wave velocity remained constant at

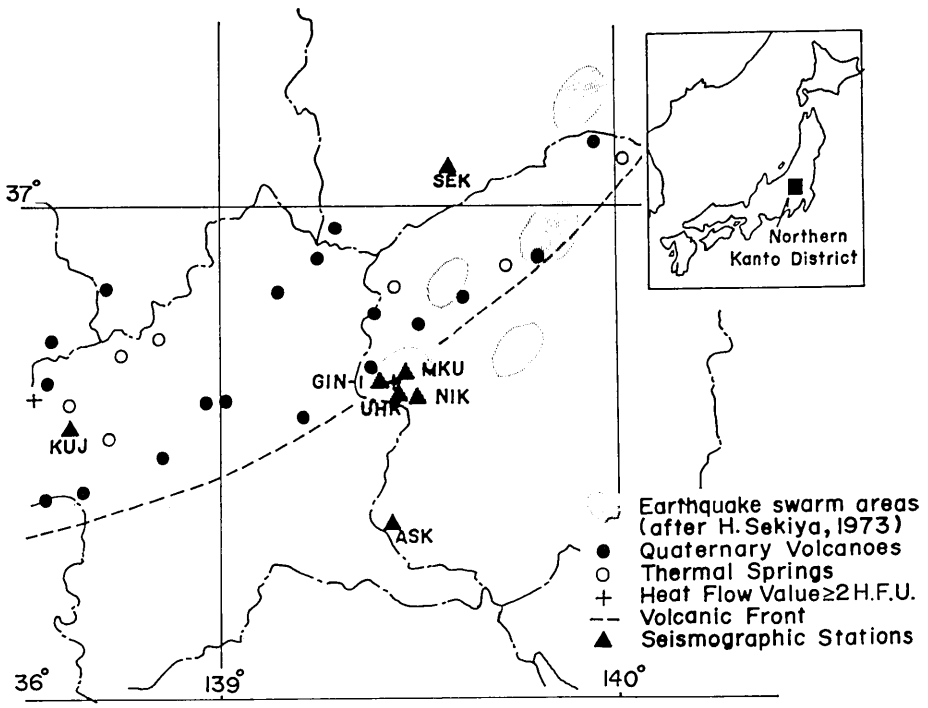

Fig. 20. Volcano-seismotectonic environment in the northern Kanto district. Earthquake swarm areas (hatched zones), Quaternary volcanoes (solid circles), thermal springs (open circles), sites of high heat flow values (crosses) and volcanic front (dashed line) are indicated with the location of the seismographic stations of NIK, UHK, GIN-1, SEK, ASK and KUJ. NIK (Nikko), SEK (Sekiya), ASK (Ashikaga) and KUJ (Kuni) are permanent stations for microearthquake observations operated by E. R. I.

5.8 km/sec and S wave velocity decreased from 3.35 km/sec to 0.00 km/sec across the discontinuity. The results support the idea that the deep crustal discontinuity are sharp and could be underlain by a material of very low rigidity.

v) It has been pointed out that the earthquake swarms are found in the geothermal or volcanic zones along the northwestern part of Tochigi Prefecture to Fukushima Prefecture. The earthquake swarms near Ashio can be classified into a typical example of this type of activity judging from the regional alignment of epicenters as shown in Fig. 20. The extremely shallow focal depths of less than 8.5 km for the earthquake swarms suggests a geothermal effect preventing an occurrence of earthquakes at a deeper part of the earth's crust. The unusual crustal discontinuity underlain by a molten material might affect earthquake activities in both ways as to supply thermal strain energy in the shallower part of the earth's crust as well as to prevent brittle fructure in the deeper part of the earth's crust.

vii) A comparison of the characteristic features of the reflections observed near Ashio with those in the Rio Grande rift leads to a conclusion that the reflections in the two different regions are nearly identical. Therefore, an existence of an extensive sill shaped magma body beneath A shio may be a plausible explanation for the reflections as confirmed in the case of the Rio Grande rift.

References

BROWN, L.D., C.E. CHAPIN, A.R. SANFORD, S. KAUFMAN and J. OLIVER, 1980, Deep structure of the Rio Grande rift from seismic reflection profiling, *J. Geophys. Res.*, 85, 4773-4800.

KAMINUMA, K., K. TSUMURA, H. MATSUMOTO and J. KARAKAMA, 1970, Micro-seismic observation at Kobugahara, Tochigi Prefecture. Aftershock observations of the earthquake, August 13, (in Japanese with English abstract). *Bull. Earthq. Res. Inst.*, 48, 53-63.

MIZOUE, M., 1971, Crustal structure from travel times of reflected and refracted seismic waves recorded at Wakayama Micro-earthquake Observatory and its substations, *Bull. Earthq. Res. Inst.*, 49, 88-92.

MIZOUE, M,. 1980, Deep crustal discontinuity underlain by molten material as deduced from reflection phases on microearthquake seismograms, (in Japanese with English abstract). *Bull. Earthq. Res. Inst.*, 55, 705-735.

OGINO, I., 1974, Seismic activity in Ashio area, Tochigi Prefecture, (in Japanese with English abstract). *Preliminary Rep. Earthq. Res. Inst.*, 12, 159-169.

OLIVER, J. and S. KAUFMAN, 1976, Profiling the Rio Grande Rift, *Geotimes*, 21, 20-23.

RINEHART, E.J. and A.R. SANFORD, 1981, Upper crustal structure of the Rio Grande Rift near Soccoro, New Mexico, from inversion of microearthquake S-wave reflections, *Bull. Seism. Soc. Amer.*, 71, 437-450.

SANFORD, A.R. and L.T. LONG, 1965, Microearthquake crustal reflections, *Bull. Seism.*

Soc. Amer., 55, 579-586.

SANFORD, A. R., O. ALPTEKIN and T. R. TOPPOZADA, 1973, Use of reflection phases on microearthquake seismograms to map an unusual discontinuity beneath the Rio Grande Rift, *Bull. Seism. Soc. Amer.*, 53, 2021-2034.

SANFORD, A. R., R. P. MOTT, JR., P. J. SHULESKI, E. J. RINEHART, F. J. CARVAELLA, R. M. WARD and T. C. WALLACE, 1977, Geophysical evidence for a magma body in the crust in the vicinity of Soccoro, New Mexico, the Earth's Crust, J. G. Heacock, Editor, *Amer. Geophys. Union, Geophys. Monogr.*, 20, 385-403.

SCHILT, S., J. OLIVER, L. JENSEN, P. KRUNHANSL, G. LONG and D. STEINER, 1979, The heterogeneity of the continental crust, Results from deep crustal seismic reflection profiling using the vibroseis technique, *Reviews of Geophys. and Phys.*, 17, 354-368.

SEKIYA, H., 1973, On the seismic activity in the southern part of Kanto (Relation between the earthquake swarms and other large earthquakes), (in Japanese), *Rep. Coord. Commit. Earthq. Pred.*, 10, 36-39.

SUZUKI, M. and H. KAMEYAMA, 1972, The seismic activity in the western part of Tochigi Prefecture (I), (in Japanese with English abstract), *Bull. Faculty of Education, Utsunomiya Univ.*, 22, 45-52.

SUZUKI, M., H. KAMEYAMA, Y. KOSHIKAWA and T. SASANUMA, 1973, Microearthquake activity in the western part of Tochigi Prefecture. (II), (in Japanese), *Abst. Seism. Soc. Jap.*, 2, 1973.

THE RESEARCH GROUP OF ACRIVE FAULTS OF JAPAN, 1980, Active faults in Japan: Sheet maps and inventories by the research group for active faults, *Tokyo Univ. Press*, 142-145.

TSUKUDA, T., 1976, Microearthquake waveforms recorded at Tottori Microearthquake Observatory and their relation to hypocentral distributions and the upper-crustal structure, *Bull. Disas. Prev. Res. Inst., Kyoto Univ.*, 26, 17-55.

30. 栃木県北西部，足尾周辺の群発地震活動地域での微小地震反射波による地殻内不連続面の検出とその特異性について

地震研究所 溝上恵
地震研究所 中村功
気象庁気象究研所 横田崇

北関東，栃木県北西部の足尾地域では浅発性の群発地震活動がみられる．この地域の微小地震の分布および地殻構造を調べるために高感度短周期地震計による4点のテレメータ方式の観測網を設置した．その観測データの解析結果を要約すると以下のようである．

i) 足尾地域の群発地震活動にともなう微小地震の空間分布は震央の集中する数ヶ所の部分からなる微細構造をもつ．とくに注目すべきことは足尾山地にみられる活断層（内ノ籠断層）にそう顕著な微小地震活動が存在することである．この断層にそう微小地震について P 波初動の重ね合せによるメカニズム解を求めると走向 N28°E，節面の傾斜角が約 35° の逆断層の存在が推定される．震源の深さは 8.5 km よりも浅い．

ii) S-P 時間が 1.5 sec 以下の微小地震を観測すると直達 S 波の後に2つの顕著な位相が検出されることがしばしばある．走時からこれらの位相は深さ 14～17 km の不連続面からの反射波 S_xP および S_xS であることがわかった．

iii) 精度の良い震源座標および反射波走時を組合せることにより足尾地域全体についての反射点の深さの分布を求めた．その結果不連続面はほぼ SE 方向に傾斜し，足尾を中心にみると 30～35° という異常なに大き傾斜角を示す．またこれらの反射波は足尾周辺の全域について一様に検出されるのではなく，きわめて限られた区域についてのみ顕著な反射波が観測されることがわかった．

iv) 反射波 S_xP および S_xS はほぼ垂直反射に近いので震源から射出されるエネルギーおよび伝播経路に大きな差はない．それにもかかわらず，SV 波についての S_xP と S_xS との振幅比は入射角の補正を行うと S_xS の方が S_xP に比較して数倍から1桁大きい．これは S 波の速度が不連続面で急激に減少することを示唆している．すなわちこの不連続面の直下では物質が部分的に溶けていると考えると都合がよい．

v) 足尾周辺の群発地震活動と類似した局地的な活動域は地熱地帯ないしは火山地帯にそって福島県の北部にまでつながっていることが指摘されている．また足尾周辺の群発地震の震源の深さはきわめて浅く 8.5 km より深いものは検出されない．このことは当地域の群発地震活動が地殻深部の熱源の存在に関連しているためかもしれない．

vi) Rio Grande Rift では Soccoro 付近で地表から約 19 km の深さに溶融物体があり，そのほぼ直上で発生した微小地震についてはこの溶融体の表面からの反射波 S_xP および S_xS が観測されている．これら Rio Grande Rift における反射波の特徴は走時，振幅比共に足尾周辺の反射波の特徴と一致する．